Measuring the Energetics of a Lithium Ion Battery in Thermal Runaway

Quintiere J.G.

University of Maryland, Department of Fire Protection Engineering, College Park, MD, USA
jimq@umd.edu

ABSTRACT

A calorimetry technique is developed to measure the energetics of an 18650 Li-ion battery in thermal runaway. The technique uses the battery as a calorimeter with temperature and mass loss measurements to analyze the energetics. Runaway is induced by heating of the battery. Only one battery is investigated over a range of heating power and state of charge (SOC). The dynamics of the battery are investigated including time events, temperature, mass lost and energies. The total energy in runaway is manifested by the internal energy stored in the battery and the enthalpy of the ejected mass. Combustion of the ejected gases is not studied here. Here a safety vent first causes the release of gases, then this is followed by the more dominant ejection during runaway. Vent times decrease dramatically with heating power. The duration of runaway decreases with the SOC, and runaway energy increases with the SOC. The total energy measured in runaway is compared to an alternative technical to show its accuracy. The need to assume a specific heat of the ejected mass in the current technique has an effect on accuracy. Also the possibility of melting in runaway is not included in the current technique.

KEYWORDS: Batteries, calorimeter, Li-ion, thermal runaway.

INTRODUCTION

Lithium ion batteries have a high electrical energy density. These batteries are used extensively in commercial products from electronics to powering automobiles. As with any new technology they can cause unanticipated safety issues. It has become well known that such batteries are prone to "thermal runaway" that can lead to fire and explosion hazards [1-3]. In general, thermal runaway is a process that is accelerated due to temperature. It involves a feedback mechanism in which the exothermic energy produces an increase in temperature, and the temperature causes an increase in the rate of energy generated. In runaway of a Li-ion battery, many exothermic decomposition reactions are triggered among its components, and modeling all of the electrical and chemical processes in runaway is very complex [4-6]. The primary hazard from the runaway of a battery is the transfer of this energy to other batteries causing a possible chain reaction, and the transfer of energy to the surrounding materials to cause fire and possible explosion in a confined system. The energy dynamics of runaway are key in the design of safety mitigation systems to prevent the consequences from runaway.

A typical Li-ion battery consists of a cathode of a lithium metal oxide on aluminum and a graphite anode on copper. The electrolyte is an organic solvent and is combustible. A plastic membrane separator, within the electrolyte, limits the ion transfer between the anode and cathode. The separator is a key failure point in the initiation of runaway. Failure can be initiated in several ways: (1) a manufacturing defect that produces dendritic growth breaking the membrane, (2) heating to cause the membrane to melt, (3) direct accidental puncture, and (4) over-charging. Failure of the membrane leads to an internal short circuit and thermal runaway.

The internal energy generated within the battery in runaway is composed of resistive heating and the sum of several exothermic decomposition reactions involving the cathode, anode and electrolyte [6]. Gases produced in early reactions pressurize the battery and are first intentionally vented by a pressure-relief device. This is followed by a more catastrophic ejection of mass during runaway. The energy output of a battery in thermal runaway is composed of (1) the internal energy from resistive heating and decomposition, (2) the thermal energy of the vented materials, and (3) potentially combustion energy of the vented gases. The vented materials can include gases composed of CO_2, CO, H_2, CH_4, other hydrocarbon and possibly a little oxygen, and solids composed of copper, graphite and molten aluminum [3]. These three energies comprise the potential fire hazard to the surroundings.

Measurement techniques have been used to measure the thermodynamic energy and the rate of energy from batteries during runaway. A commercially available technique is an adiabatic Accelerating Rate Calorimeter (ARC) but it is limited to temperature ranges well below the temperatures after the onset of runaway. In Roth et al [7] an ARC measures energy rates up to about 160 ºC. A novel technique was developed by Walters and Lyon [8] and Lyon and Walters [9] using a standard oxygen bomb device, but with an atmosphere of nitrogen. The "bomb" and ARC methods are closed systems and will measure both the energy internally generated in runaway and the energy vented from the battery. Another technique using the battery itself as a calorimeter was developed by Liu et al [10] and Said et al [11] in which they address runaway rates and energies for several Li-ion batteries. Results will be presented here for a similar battery calorimeter. These results are based on a report by Quintiere et al [12] that also included the combustion energy as measured in a combustion calorimeter [13].

BATTERY CALORIMETER DESIGN

The calorimeter design is based on an energy balance for the battery. An 18650 battery (18 mm in diameter and 65 mm in length) was considered without its plastic covering. Although the battery is a cylinder, its internal battery element consists of a thin rectangular battery pouch wound into a cylindrical shape. A measurement of the battery temperature and its mass over time in runaway is used to compute the various energy components. The battery is heated by a wrapped powered Nichrome wire to induce runaway. An electric arc is used to ignite the escaping gases at the battery's vented end. A holder for the battery consisted of a tight thin copper sleeve (0.6 mm), covered by thin ceramic paper with a winding of Nichrome heating wire around its outside. Power (*P*) to the wire was measured by current and voltage. The entire battery and holder assembly is continuously weighed; and temperature is measured by a flattened thermocouple sandwiched between the copper sleeve and the outer steel shell of the battery. The entire battery and holder is wrapped in thick low density (48 kg/m^3) ceramic blanket and jacketed by a steel 70 mm diameter cylindrical shell. The components of the assembly are illustrated in Fig. 1. A schematic is shown in Fig. 2.
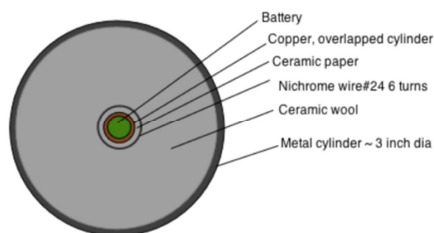

Fig. 1. Calorimeter components.

Fig. 2. Schematic of calorimeter.

CALIBRATION OF CALORIMETER

The battery calorimeter is calibrated by using an energy balance with a solid aluminum cylinder identical in size to the 18650 batteries. The specific heat of the aluminum is taken as 1.05 kJ/(kg·K) at 125 °C. A control volume (CV) is selected to encompass the aluminum cylinder, copper and ceramic paper sleeves, and the nichrome heating wires. Heat is lost from the control volume to surroundings comprising the ceramic blanket wool and the exiting electrical wires for power. The aluminum is inert so the mass of the CV-contents is constant and taken as that of copper (21.5 g) and aluminum (47 g). The masses of the ceramic paper and the 24 AWG (0.5 mm diameter and 46 cm in length) resistance wire are neglected. Applying the conservation of energy to the CV with the following assumptions: (1) the battery and copper cylinder are considered thermally thin at the same homogeneous temperature, and (2) the heat loss rate ($\dot{Q}_{loss}$) is by conduction into a semi-infinite media, gives

$$\left[(mc)_{Cu} + (mc)_{Al} \right] \frac{dT}{dt} = P - \dot{Q}_{loss} \,. \tag{1}$$

The heat loss rate to the ceramic insulation and from the wires is assumed to be of the form

$$\dot{Q}_{loss} = \beta (T - T_i) / \sqrt{t} \,. \tag{2}$$

The specific heat of aluminum was derived from the calorimeter analysis and compared to its literature value. The analysis used $\beta = 1.4$ W·s$^{1/2}$/K and a specific heat for copper of 0.39 kJ/(kg·K) in two repeated tests each with a power input of 26.4 W. Figure 3 shows the computed specific heat for aluminum. For early times and for corresponding low temperatures, the thermally thin assumption is not appropriate. However, as the heat loss is small in this early period, the aluminum calorimeter appears to give a good calculation for its specific heat.
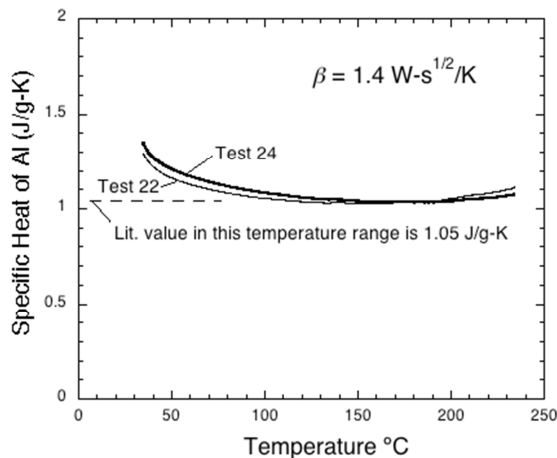

Fig. 3. Calibration of the calorimeter using an aluminum battery surrogate.

BATTERY

In this study only one battery was tested. It was a Li-ion 18650 battery with a LiCoO$_2$ cathode having a nominal 3.7 V and 2600 mA-hr rating. This gives a nominal maximum stored energy of 34.6 kJ. The battery mass was 44.2$\pm$0.1 g over the series tested in which the power input to initiate runaway was varied from about 10 to 74 W, and the State of Charge (SOC) was varied from about 0 to 100 %. Here the SOC is found by a discharge of the battery from its rated capacity.

Temperature uniformity of battery

Several tests were made to investigate the assumption of the battery and copper sleeve as thermal thin and uniform in temperature at any time. The internal battery temperature was measured at its axial and lateral center along with the normal calorimeter temperature measured on the outer center of the battery between it and the tight fitting copper sleeve. Figure 4a shows the results. Also Figure 4b shows the results for the outer center and end of the battery in another test. The results indicate that the battery temperature is reasonably homogeneous within about 20 ºC, however there is an anomaly for the center-outer temperature after runaway. From Figure 4a it can be seen that there is a delay in response to the outer battery shell of about 20 s and about 60 s for the interior of the battery. So the thermally thin assumption for the system is reasonable after 60 s.
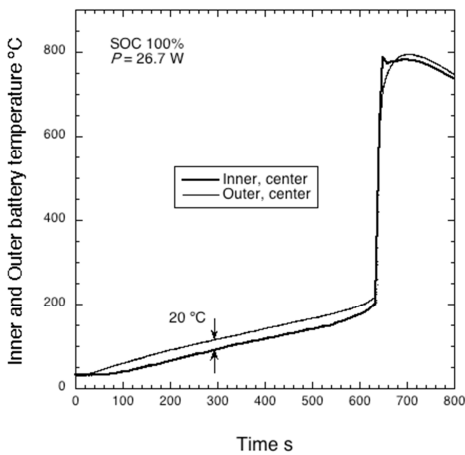

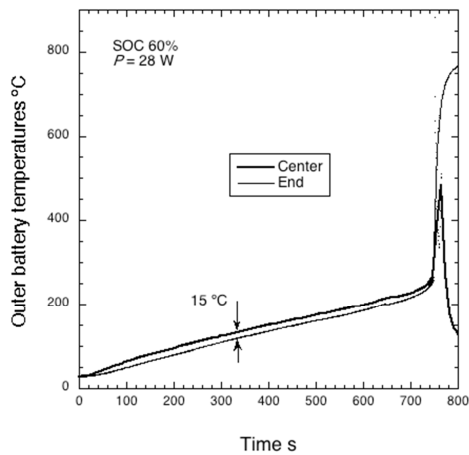
Fig. 4a. Temperature within battery and outer shell.   **Fig. 4b.** Outer center and end temperatures.
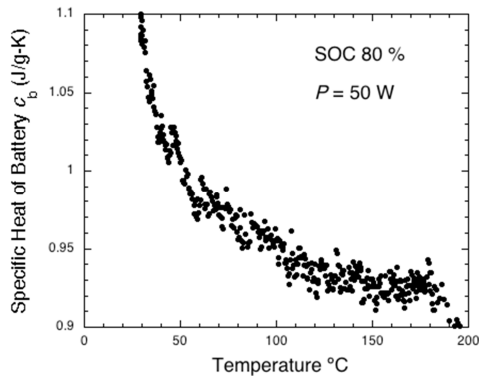

Fig. 5. Typical determination of the battery specific heat before runaway.

Specific heat of battery

The specific heat of the battery was determined for each thermal runaway experiment during the inert battery phase before runaway. This inert period was primarily below 200 ºC for this battery. Equation (1), with the battery substituted for the aluminum, was used to reduce the data. Figure 5 shows a typical determination for the battery specific heat. The inaccuracy below about 100 ºC is due to the delayed temperature response of the battery. The specific heat did not significantly vary over the range of testing this battery and was found to be 0.95±0.03 kJ/(kg·K). This value was taken as constant for all analyses in the tests, in spite of mass lost from the battery during runaway.

MODELING THE DYNAMICS OF BATTERY RUNAWAY

In these tests runaway was induced by heating of the outer battery. The heating power was varied in the tests as well as the SOC of the battery. The heating likely melted of the plastic membrane separator and caused an internal electrical discharge and runaway. This electrical and chemical energy is manifested within the battery as a generation term $\dot{Q}_b$, and outside of the battery by an ejection term of enthalpy from the battery. The conservation of mass for the system CV yields that the rate of mass ejected is equal to the rate of change for the battery mass, m. As shown in [14], the conservation of energy states that the rate of internal energy plus the rate of ejected enthalpy is equal to the sum of the heating power (P) and the generation term ($\dot{Q}_b$) minus the heat loss into the ceramic wool ($\dot{Q}_{loss}$) given by Eq. (2). Rearranging to solve for the internal generation term gives

$$\dot{Q}_b = (mc)_{Cu}\frac{dT}{dt} + c_b\frac{d(mT)_b}{dt} + \dot{Q}_{loss} - P - c_g T\frac{dm}{dt}. \tag{3}$$

The values for the constants in Eq. (3) are: $(mc)_{Cu}$ = 8.4 J/K, c_b = 950 J/(kg·K), and c_g is assumed as 1050 J/(kg·K). The value of the specific heat for the ejected materials is selected for expedience as their components are not known and can comprise gases of hydrogen, carbon dioxide, methane and others, as well as possibly molten aluminum. At 1000 K, the specific heats of hydrogen, carbon dioxide and methane are respectively, 15000, 1200 and 4500 J/(kg·K). Therefore the uncertainty of the specific heat for the ejected mixture as well as ignoring any possible melting leads to an underestimation for this ejected energy term defined as

$$\dot{Q}_g \equiv c_g T\frac{dm}{dT}. \tag{4}$$

It will be shown that the battery undergoes very rapid changes during runaway. As a consequence the computation of time derivatives from the temperature and mass measurements can be problematic. Moreover the practical manner to assess the hazard of the battery in runaway is not to have the precise rate of energy released, but to have the total energy, realizing this is a potential transfer to the surroundings in a short time. Therefore, Eq. (3) is integrated to obtain the energy released over time

$$\int_0^t \dot{Q}_b dt = Q_b = (mc)_{Cu}\left(T - T_i\right) + c_b\left(mT - m_i T_i\right) + \int_0^t \dot{Q}_{loss} dt - Pt - c_g\int_{m_i}^m T dm, \tag{5}$$

with the ejected energy as $Q_g \equiv c_g\int_{m_i}^m T dm$. Equation (5) will be used to reduce the data for a series of tests on the battery varying SOC and P. In all the tests the heating power was initiated at the start and kept constant throughout the test. An electric arc was manually initiated at the start of venting to attempt to ignite the gases. This was not always successful due to timing and location, and at times auto ignition could occur before the arc was struck.

TYPICAL DATA AND ANALYSES

Test 17 using a heating power of 25.6 W and a SOC of 100% is examined to show the typical results for this battery. The raw data of battery temperature and mass are shown in Figure 6. There is a nearly linear rise in temperature until about 500 s when the pressure safety vent opens and releases white vapors. In general these vapors could be ignited but ignition was not achieved in this test at the first vent. These vapors continue to vent until about 550 s where thermal runaway occurs. The feedback between battery temperature and decomposition takes place over several seconds.

This is seen as a nearly vertical jump in temperature and drop in battery mass. Runaway is a violent process with a high velocity jet from the pressure safety end of the battery. This ejection is about 35% of the original battery mass. In several seconds the battery temperature jumped from about 200 ºC to 800 ºC. Runaway is a dramatic event.
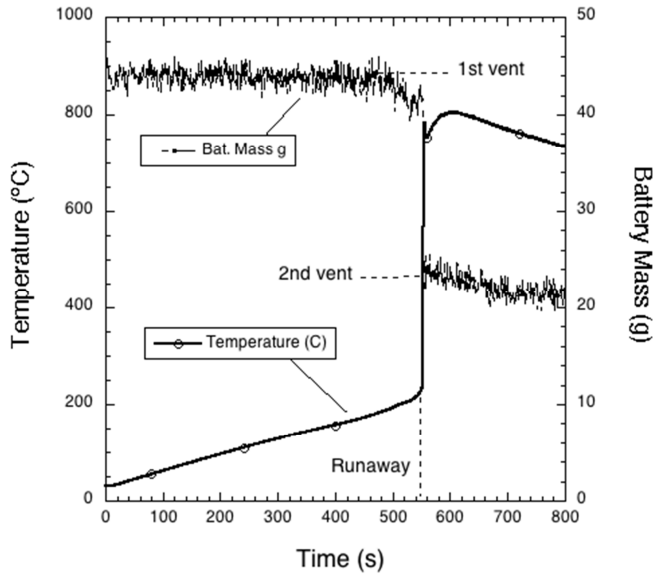

Fig. 6. Battery temperature and mass at 100% SOC and heating power at 25.6 W.
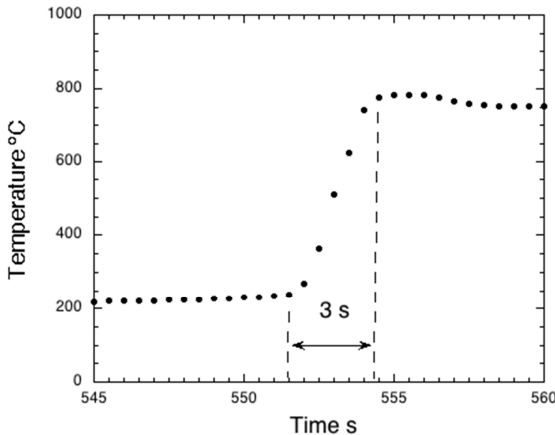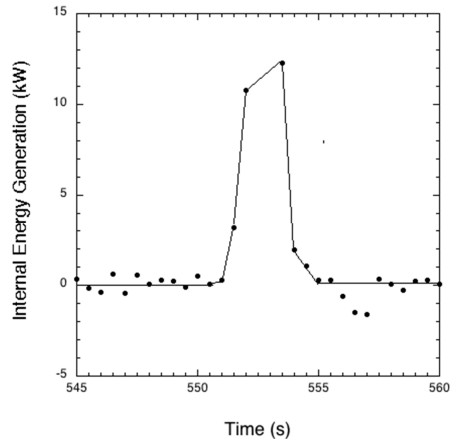

Fig. 7. Temperature at jump.

Fig. 8. Internal generation rate of energy.

The runaway event is examined more closely over the jump period (551.5 to 554.5 s). Figure 7 shows the temperature jump and Fig. 8 shows the rate of internal energy computed, $\dot{Q}_b$. The dramatic jump in 3 seconds shows the characteristic of thermal runaway in a battery. While the rate of internal energy generation can be computed, its distribution over time may not be as significant as the total energy dumped in this process. However ejected energy from the battery commenced at the first vent (~ 500 s) at about 190 ºC; then most of this category of energy was released during the jump after the second vent (~ 550 s). Consequently most of the battery energy converted from its original electrochemical energy is primarily transferred in this jump period, and will be represented by Q_b and Q_g over the entire heating period of the battery as given in Eqns. (4) and (5).

Figure 9 shows the specific energy terms in Eq. (5) individually computed for Test 17. As Q_b is computed from the algebraic sum of the RHS terms some inaccuracy can be noted as its value is about –1.5 kJ before the jump instead of zero. However after the jump this internal energy computed is 30 kJ. Q_g reaches about 18 kJ. Therefore the total energy of the battery released during runaway is about 48 kJ, compared to its rated energy at 100 % SOC of 34.6 kJ. Of course this does not include the combustion energy that can be released if the vented gases are ignited.
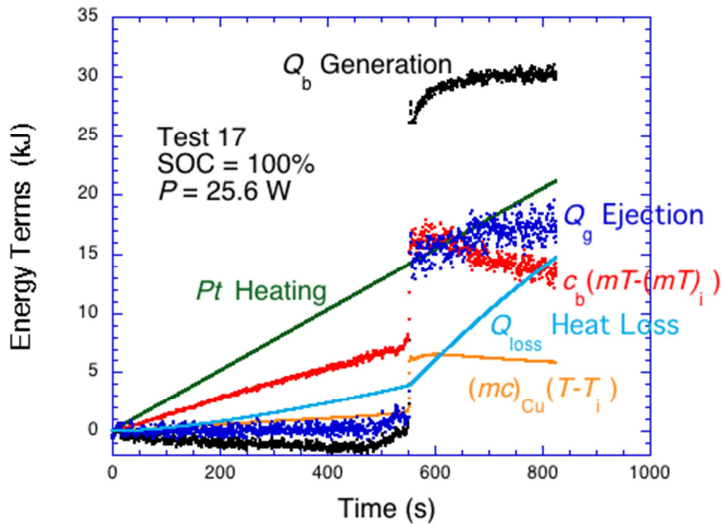
Fig. 9. Battery energy terms over time.

OVERALL RESULTS DEPENDENCE ON SOC AND HEATING POWER

About 25 tests were made with the same battery to assess the effects of the heating power the SOC. It might be expected that energy in runaway would be related to the electrical energy stored, and that the heating power should affect the time to runaway.

EFFECT OF HEATING POWER

In this series the battery SOC was maintained at 80% and the heating power varied from about 10 to 74 W for the duration of each test. The heating power reduces the time for runaway, as the safety vent operation and for the second venting at thermal runaway both decrease with heating (Fig. 10). In the configuration of the battery in the calorimeter, all heating powers were able to initiate runaway. The duration of the runaway event varied from 3 to 12 s without a definite trend with the heating power.

Although the times for venting and runaway varied significantly, the associated temperatures only varied slightly. Figure 11 shows these slight trends where the trigger temperature for runaway is about 220 to 300 ℃. During runaway the temperatures rise to over 750 ℃ in 3 to 12 s. This rapid rise is indicative of the battery hazard in thermal runaway. Figure 12 shows the mass loss fractions of the battery after the first safety vent and the runaway vent occur. The mass loss fractions are not significantly dependent on the heat power. About 10% of the original mass is ejected during the safety venting and up to 40% is lost after runaway. This indicates that more hot stuff is ejected following runaway, and much of this is combustible.

Figure 13 shows a slight effect of heating power on the internal energy and on the ejected energy.

The former is about 30 to 35 kJ for this 80% SOC and the latter is about 10 to 18 kJ. Hence heating power significantly effects the time for venting and runaway, but not significantly the vent and runaway temperatures, and mass ejected and energy produced.
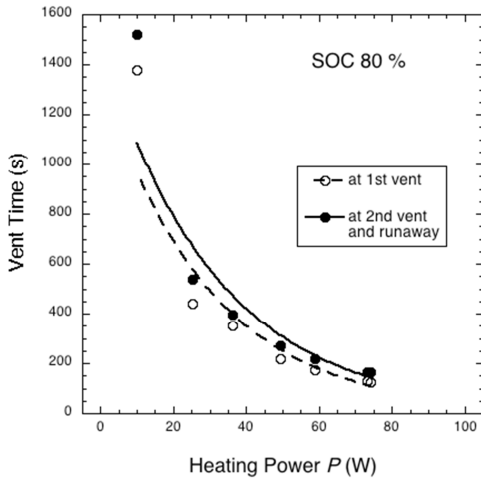
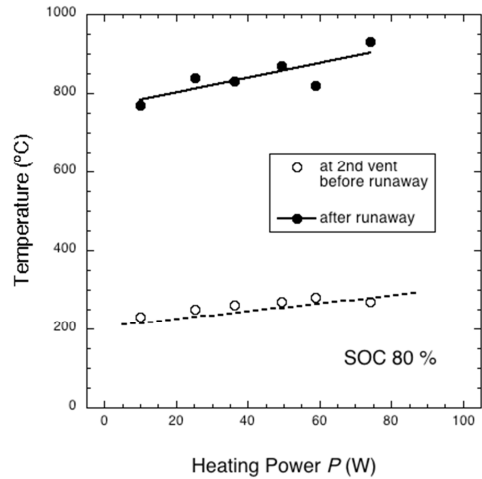

Fig. 10. Vent times as a function of heating.

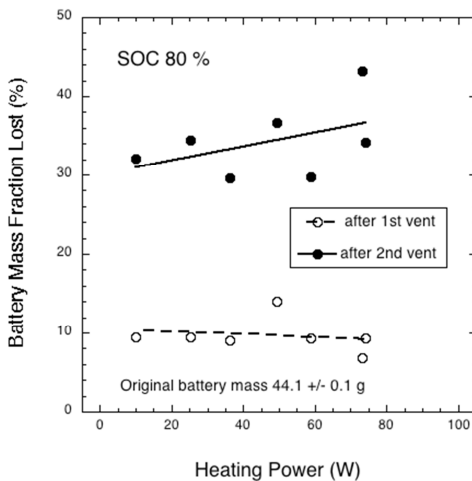**Fig. 11.** Temperature at onset and after runaway.
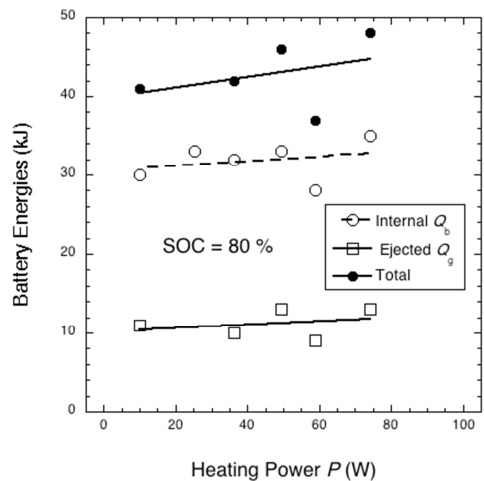

Fig. 12. Battery mass lost at venting.

Fig. 13. Battery runaway energies vs heating rate.

EFFECT OF STATE OF CHARGE

The effect of SOC is now examined. Here the heating power is essentially constant for all the tests at about 25 ± 2 W. Figure 14 shows the times to safety vent (1st) and runaway (2nd) are nearly invariant with SOC. The temperatures at of the 1st vent and the onset runaway are also invariant with SOC, but the final temperature of the battery increases with the SOC (Fig. 15). The 1st vent temperature is indicative of the designed pressure relief vent configuration, and is due solely to the heating power. The 2nd vent temperature is indicative of the onset of thermal runaway that depends on the battery and its heat loss environment. The temperature after runaway depends on the internal energy remaining in the battery and its ejected energy.
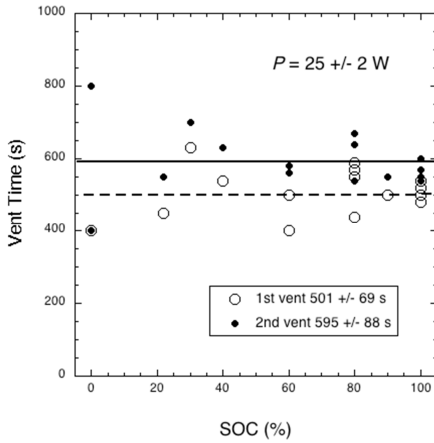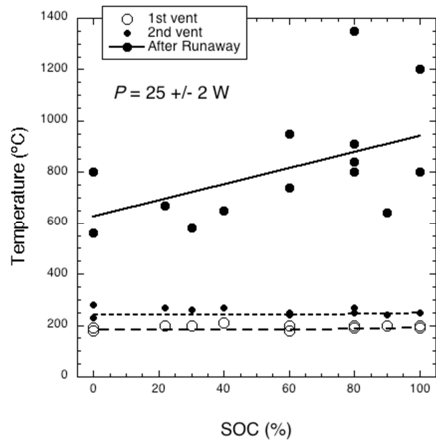
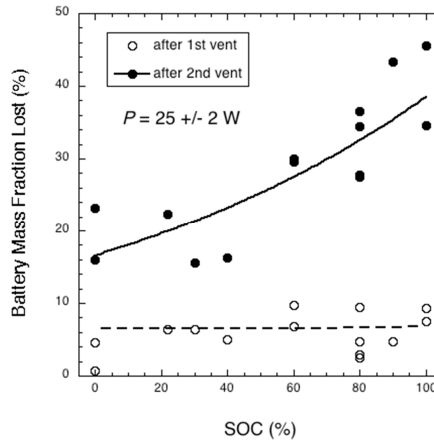**Fig. 14.** Vent times vs SOC.

Fig. 15. Temperature vs SOC.

Fig. 16. Battery mass vs SOC.
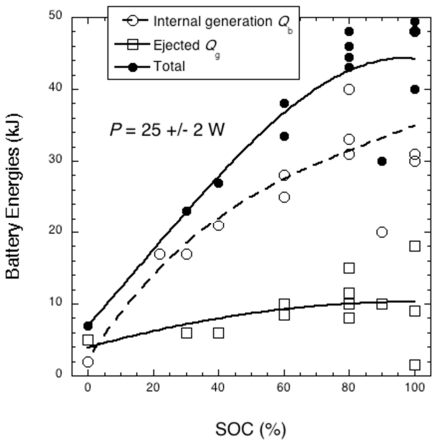

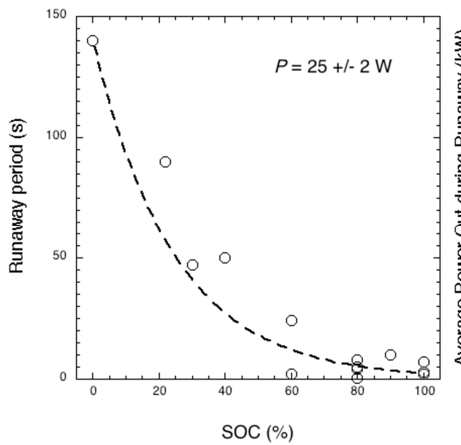**Fig. 17.** Battery energies vs SOC.
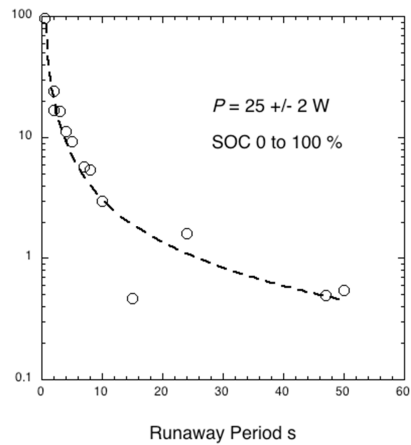

Fig. 18. Runaway time period vs SOC.

Fig. 19. Average runaway power vs runaway period.

Figures 16 and 17 show that, at runaway, the mass ejected and the energies released (internal and ejected) are directly related to the SOC. If runaway is perceived as an internal short circuit, then a

portion of the original battery energy would be represented as resistance heating. As the remaining portion of the energy is due to decomposition dependent on temperature then it too will increase with SOC as Fig. 15 shows the temperature after runaway increases with SOC. As the mass ejected increases after runaway, so does the combustion potential hazard of these gases.

Here the "runaway period" is defined as the time increment from just after the onset of runaway to just before the end of runaway as indicated by battery temperature. The runaway period decreases dramatically with SOC – from nearly 100 s at 20% to as low as 0.5 s at 80% at which the runaway temperature nearly reached 1400 °C (Figs. 15 and 18). The average runaway power in this period can be computed from the total energy released. Figure 19 shows how this varies with the runaway period. Nearly 100 kW can be released in ½ second!

DISCUSSION OF RESULTS

For this thermally induced runaway in a battery, the SOC has a strong dependence on the battery hazard. Studies have also found this increase in hazard with SOC for other Li-ion batteries [8-12]. Figure 20 shows a comparison of the current results for the same battery with Liu et al [10], along with their combustion energy measured in the Cone [13]. Similar decreases in combustion energy at high SOC were also noted for other batteries [12]. The heat of combustion of the ejected gases was found to range from about 1 to 18 kJ/g for various batteries [12].

The accuracy of the current results can be tested by a technique developed to measure the overall energy [8] that used an Oxygen Bomb apparatus but with an atmosphere of nitrogen. A comparison of their results with the total energy measured here for the same battery is shown in Fig. 20. Recall that a weakness of the current method is the uncertainty of the specific heat of the material ejected, and no consideration in the analysis for melting. The "Nitrogen Bomb" is more accurate in capturing the total energy released, especially above 80% SOC. The total energy is approximately 2 times higher than the corresponding rated energy at the SOC. Also the variation in the results for a given SOC could be attributed to the chaotic nature of runaway.
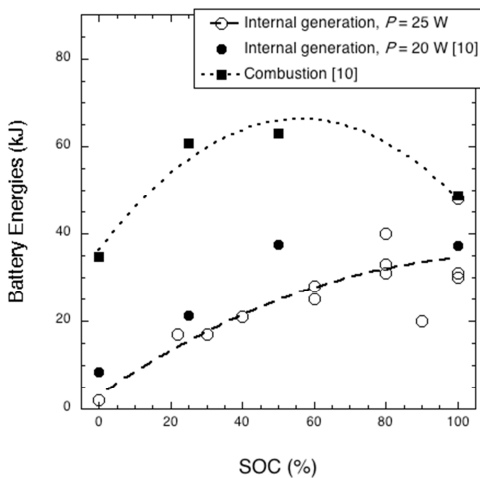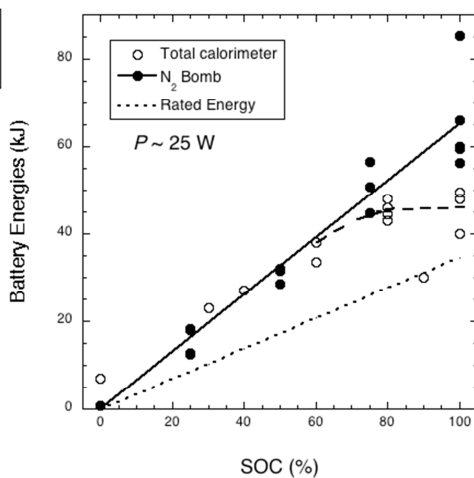

Fig. 20. Current method with Liu et al [10].   **Fig. 21.** Current method with nitrogen bomb [8].

CONCLUSIONS

The hazard of a Li-ion battery is shown to increase with the SOC. The hazard as measured here is composed of the sudden release of energy to produce a very hot battery and the ejection of hot material containing combustibles.

ACKNOWLEDGEMENTS

REFERENCES

[1] H. Webster, Flammability Assessment of Bulk-Packed, Rechargeable Lithium-Ion Cells in Transport Category Aircraft, Report No. DOT/FAA/AR-06/38, Federal Aviation Administration, 2006.

[2] H. Webster, Fire Protection for the Shipment of Lithium Batteries in Aircraft Cargo Compartments, Report No. DOT/FAA/AR-10/31, Federal Aviation Administration, 2010.

[3] C. Mikolajczak, M. Kahn, K. White, R.T. Long, Lithium-ion Batteries Hazard and Use Assessment, Report No. 1100034.000/A0F0/0711/CM01, The Fire Protection Research Foundation, 2011.

[4] D.H. Doughty, P.C. Butler, R.G. Jungst, E.P. Roth, Lithium Battery Thermal Models, J. Power Sources 110 (2002) 357-363.

[5] R. Spotnitz, J. Franklin, Abuse Behavior of High-power, Lithium-ion Cells, J. Power Sources 113 (2003) 81-100.

[6] Q. Wang, P. Ping, X. Zhao, G. Chu, J. Sun, C. Chen, Thermal runaway caused fire and explosion of lithium ion battery, J. Power Sources 208 (2012) 210–224.

[7] E.P. Roth, D.H. Doughty, Thermal Abuse of High-power 18650 Li-ion Cells, J. Power Sources 128 (2004) 308-318.

[8] R.N. Walters, R.E. Lyon, Measuring Energy Release of Lithium-ion Battery Failure using a Bomb Calorimeter, Report No. DOT/FAA/TC-TN16/22, Federal Aviation Administration, 2016.

[9] R.E. Lyon, R.N. Walters, Energy Release by Rechargeable Lithium-Ion Batteries in Thermal Runaway, Report No. DOT/FAA/TC-TN15/34, Federal Aviation Administration, 2016.

[10] X. Liu, Z. Wu, S.I. Stoliarov, M. Denlinger, A. Masia, and K. Snyder, Heat Release Rate During Thermally-Induced Failure of a Litium Ion Battery: Impact of Cathode Composition, Fire Saf. J., 85 (2016) 10-22.

[11] A.O. Said, C. Lee, X. Liu, Z. Wu, S.I. Stoliarov, Simultaneous Measurement of Multiple Thermal Hazards Associated with a Failure of Prismatic Lithium Ion Batteries, Combustion, Proc. Combust. Inst. 37 (2018) 4173-4180.

[12] J.G. Quintiere, S. Crowley, R.N. Walters, R.E. Lyon, D. Blake, Fire Hazards of Lithium Batteries, DOT/FAA/TC-TN15/17, Federal Aviation Admin. William J. Hughes Technical Center, Atlantic City Int. Airport, NJ 08405, February 2016.

[13] ASTM E7354-04a, Standard Test Method for Heat and Visible Smoke Release Rates for Materials and Products Using an Oxygen Consumption Calorimeter, ASTM International, West Conshohocken, 2004.

[14] J.G. Quintiere, Fundamentals of Fire Phenomena, John Wiley and Sons, Ltd., Chichester, 2006.